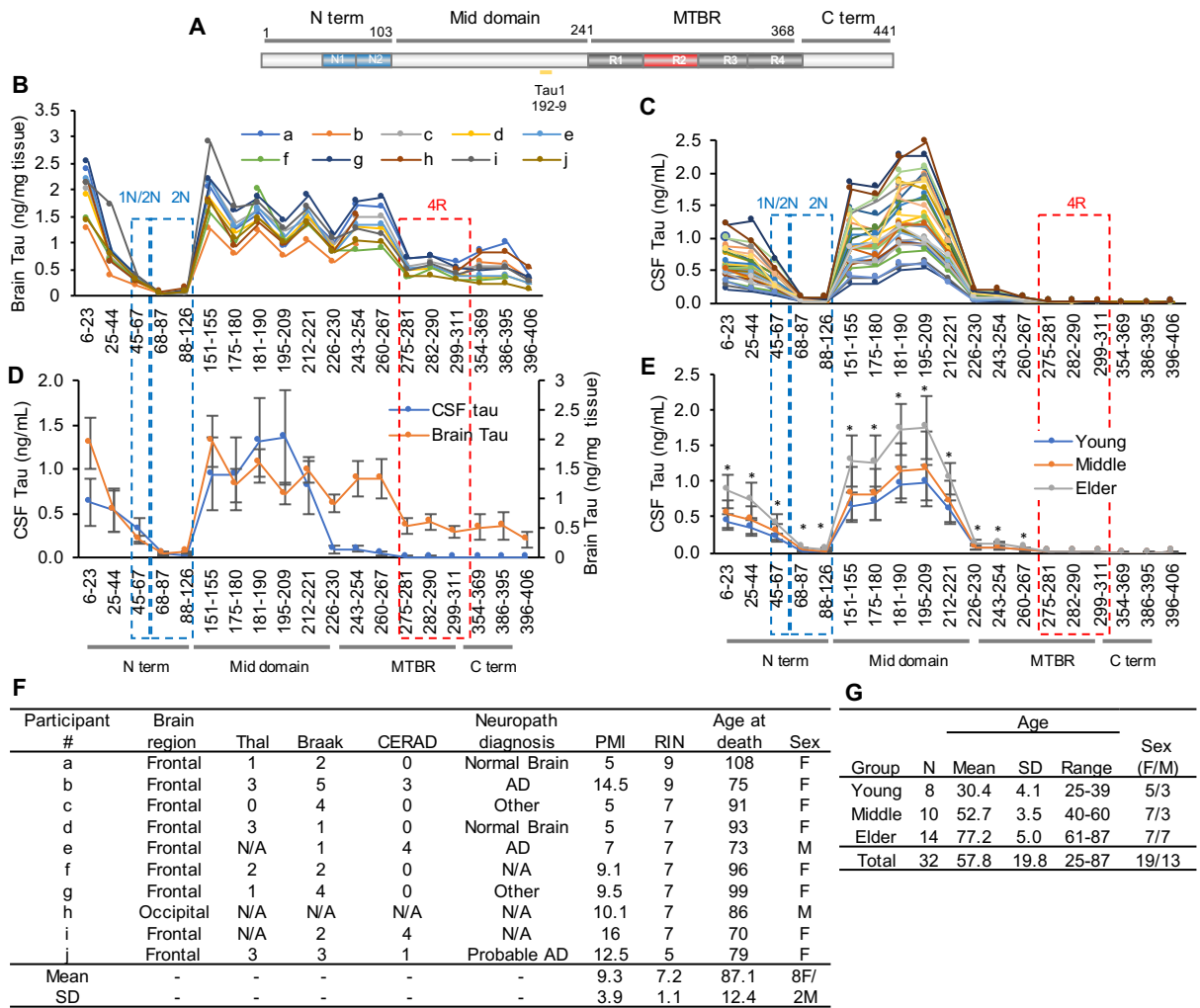


**Neuron, Volume 97**

## **Supplemental Information**

### **Tau Kinetics in Neurons and the Human Central Nervous System**

**Chihiro Sato, Nicolas R. Barthélemy, Kwasi G. Mawuenyega, Bruce W. Patterson, Brian A. Gordon, Jennifer Jockel-Balsarotti, Melissa Sullivan, Matthew J. Crisp, Tom Kasten, Kristopher M. Kirmess, Nicholas M. Kanaan, Kevin E. Yarasheski, Alaina Baker-Nigh, Tammie L.S. Benzinger, Timothy M. Miller, Celeste M. Karch, and Randall J. Bateman**



**Figure S1. Tau Profiles in 10 Human Brains and CSF from 29 controls. Related to Figure**

1. (A) Schematic of the longest tau isoform (2N4R), fragments detected by MS, and epitopes of Tau1 antibody. Absolute quantitation of tau peptides in 10 human brains (B), CSF from 29 normal controls (C), and comparison of the average of each (D). (E) CSF tau profiles from Young (age 25-39), Middle (age 40-60), and Elder (age 61-87) populations suggest that CSF tau is significantly higher in Elder compared with Middle ( $p=0.11$ ,  $F=9.28$ ,  $Df=26$ ) and Young ( $p=0.0012$ ,  $F=9.28$ ,  $Df=26$ ). The relative abundance of tau peptides remains similar.  $*p<0.05$  for Elder vs Young, and Elder vs Middle. Significance was determined via one-way ANOVA with

Tukey posthoc test. Data are represented as mean  $\pm$  SD. (F) Thal, Braak, and CERAD staging were used to assess amyloid deposition, neurofibrillary tangle, and neuritic plaque score, respectively. PMI, post mortem interval. RIN, RNA integrity number. (G) Summary of CSF used in (C) and (E).

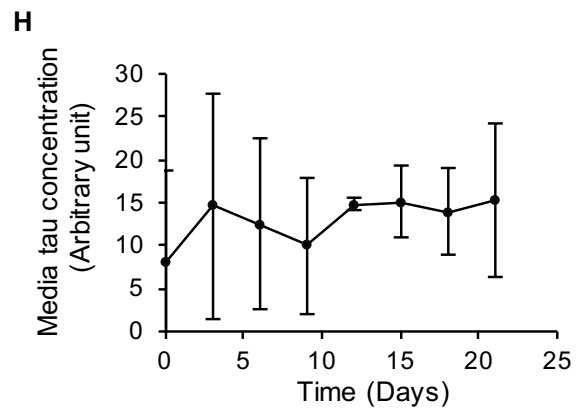
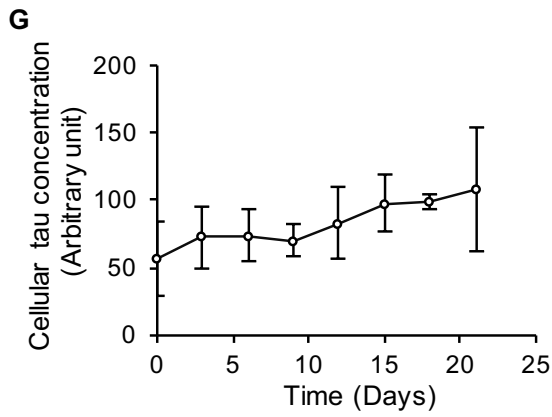
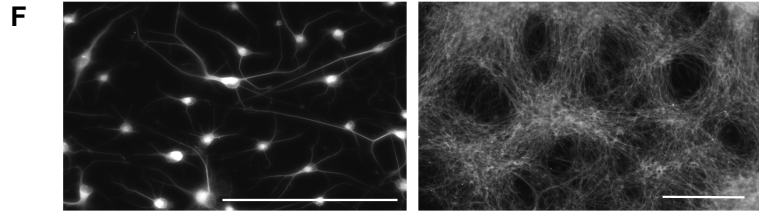
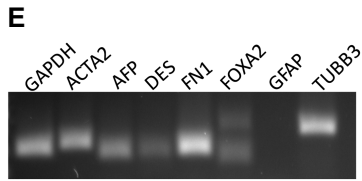
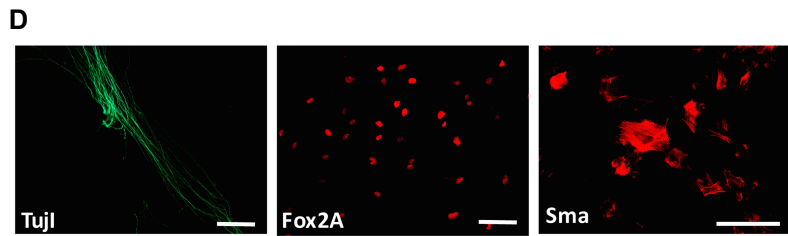
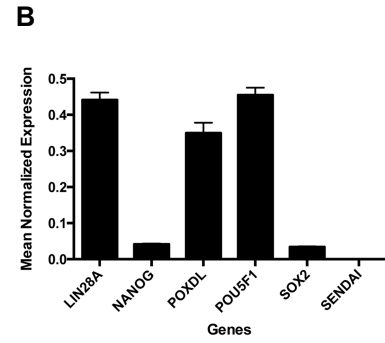
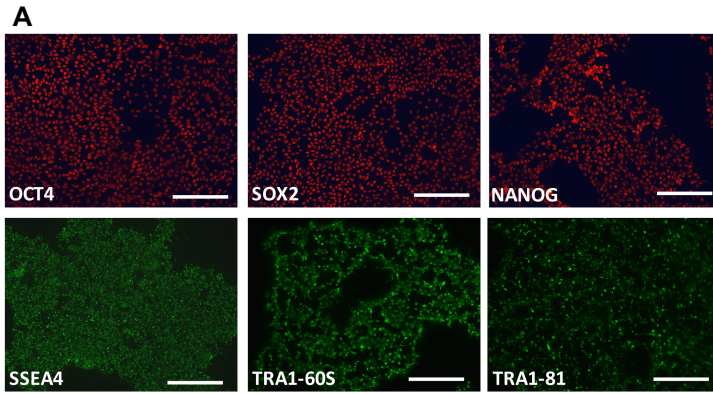


**Figure S2. Characterization of iPSCs and iPSC-derived neurons. Related to Figure 1, 2.**

Human dermal fibroblasts were reprogrammed into iPSCs using non-integrating Sendai virus.

(A) iPSCs express markers of pluripotency. (B) Quantitative PCR. Probes specific to Sendai virus-driven pluripotency genes demonstrate that Sendai virus has been diluted out of the clones. (C) Normal karyotype for iPSCs. iPSCs were cultured in DMEM/F12 supplemented with FBS to form embryoid bodies. Embryoid bodies were then plated and analyzed by immunocytochemistry (D) and qPCR (E) to demonstrate that the iPSC can spontaneously form cells from any of the three germ layers. iPSC-derived neurons express markers of neuronal cell fate and produce steady-state levels of tau (F-H). iPSC-derived neurons were stained with TuJ1. (F, left) 20x magnification. (F, right) 10x magnification. Absolute quantitation of tau using mass spectrometry in the cells (G) and media (H) from iPSC-derived neurons during 21 days of labeling starting at 4 weeks in culture. Data are represented as mean  $\pm$  SD.

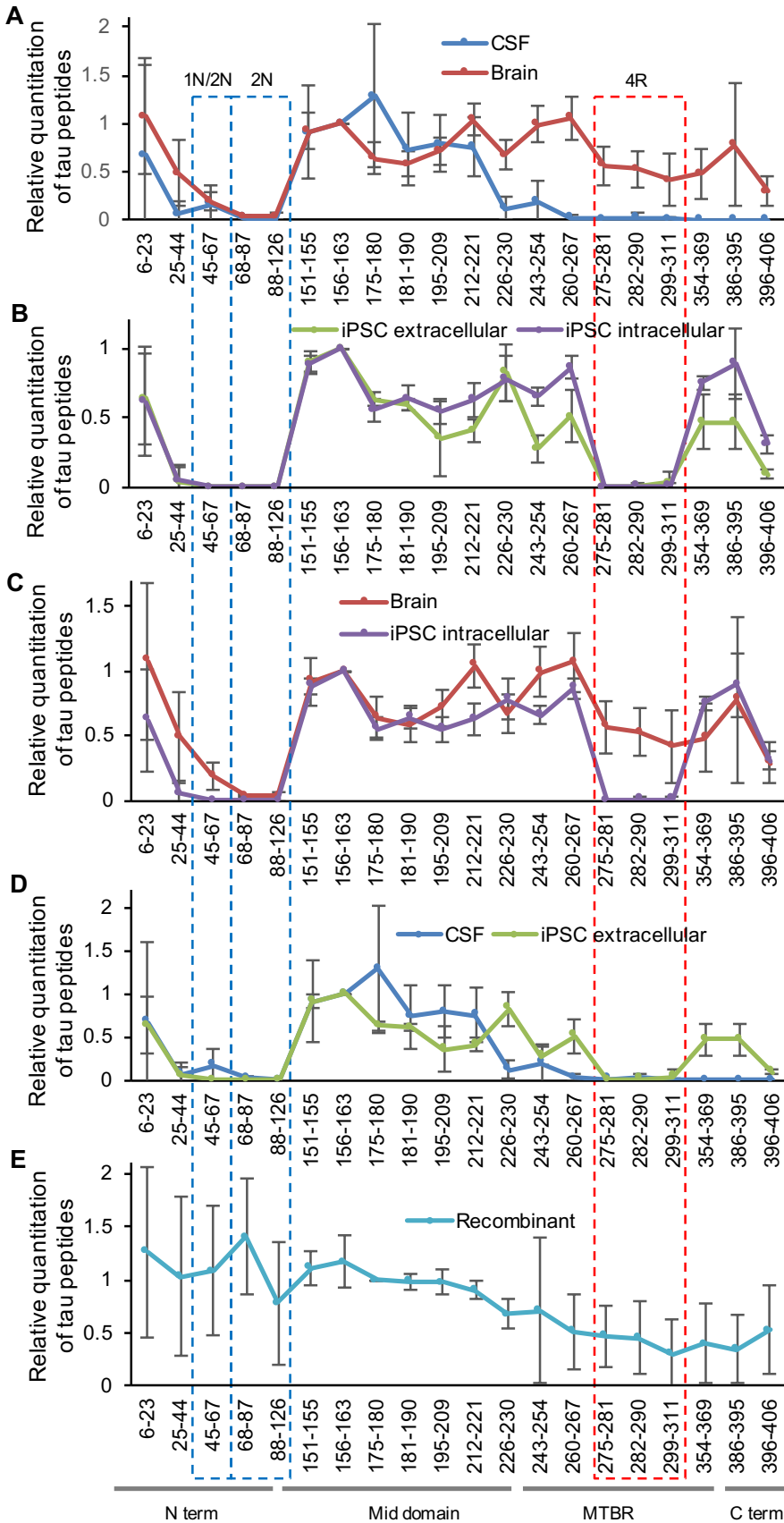


**Figure S3. Relative quantification of tau in the human brain, CSF, and iPSC-derived neurons. Related to Figure 1.** Analyses of tau using the merged results from the eight different immunopurification averaged and normalized by the signal from peptide 156-163. Comparison of tau profiles between (A) human brain vs CSF, (B) intracellular vs extracellular tau from iPSC-derived neurons, (C) human brain vs intracellular tau from iPSC-derived neurons, and (D) CSF tau vs extracellular tau from iPSC-derived neurons are shown. (E) Relative amount of recombinant tau recovered from tau antibodies reflects immunoprecipitation efficiencies and mass spectrometry quality within the domains defined. Data are represented as mean  $\pm$  SD.

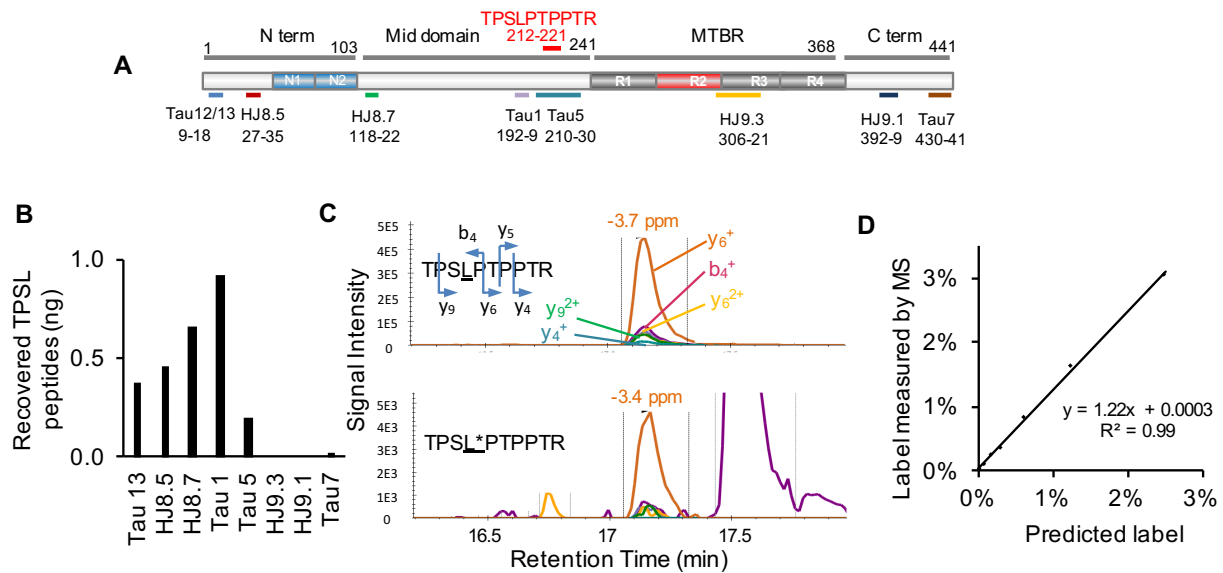


**Figure S4. Tau SILK method development. Related to Figure 2, 3.** (A) Schematic of 2N4R full length tau, epitopes of Tau antibodies, and TPSTLPTTPTR peptide. (B) IP/MS efficiencies of Tau antibodies in the normal control CSF assessed by mass spectrometry. (C) Examples of LC-MS/MS signals from TPSTLPTTPTR (unlabeled, top) and TPSTL\*PTTPTR (labeled, bottom) peptide obtained from  $^{13}\text{C}_6$ -leucine labeled samples. Approximately 1% of total tau is labeled. (D) Standard curve of TPSTLPTTPTR peptides showing the limit of quantitation of 0.1%.



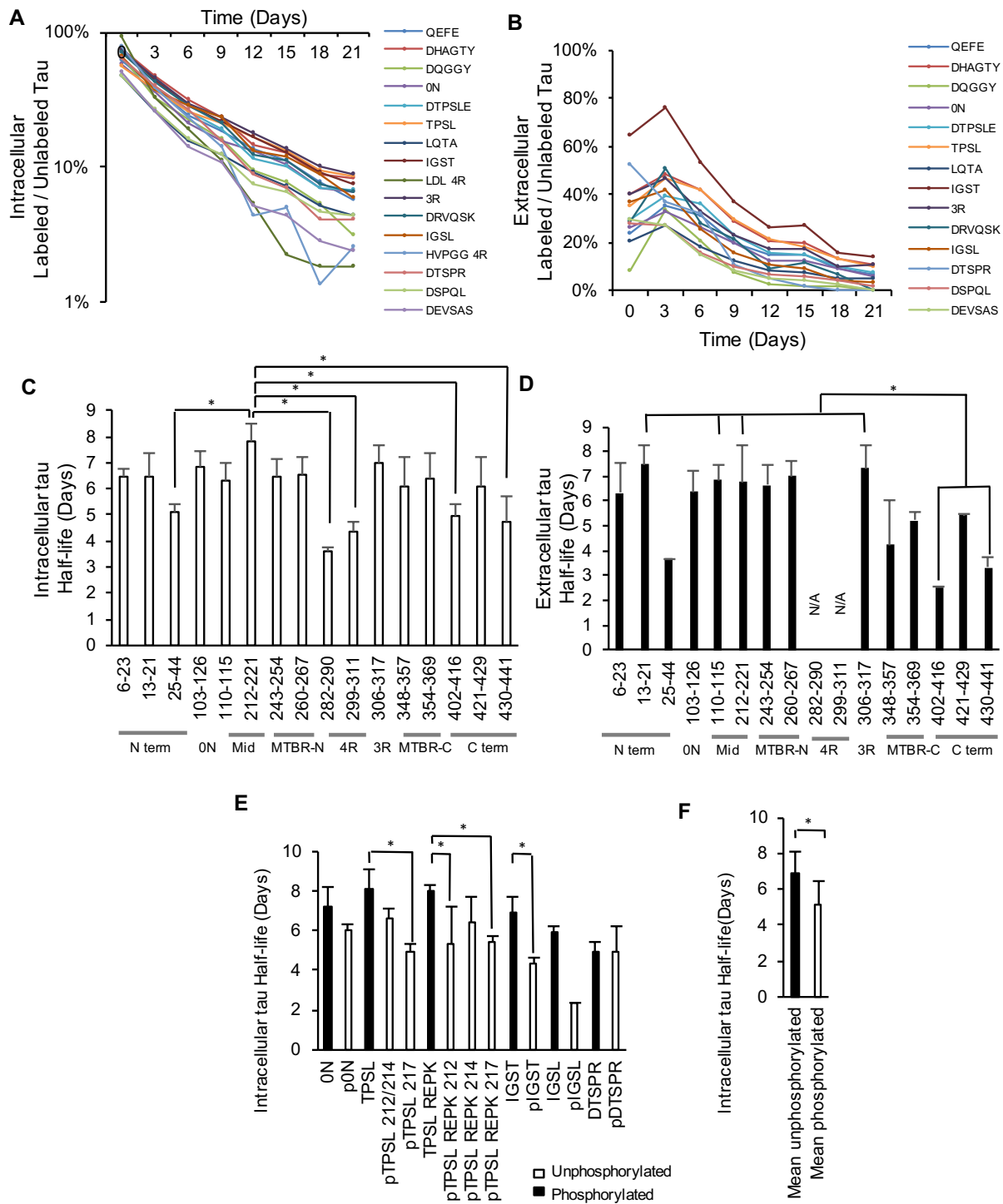


**Figure S5. Tau Kinetics in iPSC-derived neurons. Related to Figure 2, Table 1, 2.** SILK curves and half-lives of tau peptides of iPSC-derived neurons in the cells (A, C; intracellular) and in the media (B, D; extracellular), respectively. See **Tables 1 and 2** for peptide abbreviations. (C) In intracellular fraction, DQGGYT peptides (residue 25-44), 4R specific peptides (residues 282-290 and 299-304), and C term peptides (residues 402-407 and 430-441) were significantly shorter than TPSLPTPPTTR peptides (residue 212-221) (\* $p \leq 0.05$ ,  $F=5.455$ ,  $Df=29$ ). (D) In extracellular tau, C term peptides (residues 402-416 and 430-441) were significantly shorter than N term to MTBR-C peptides (residues 13-21, 110-115, 212-221, and 306-317 (\* $p \leq 0.05$ ,  $F=4.596$ ,  $Df=22$ )). (E-F) Graph summarizing the half-lives of phosphorylated and unphosphorylated tau peptides. Phosphorylated tau peptides have significantly shorter half-lives than their unphosphorylated pair. TPSL p217 ( $p=0.0057$ ,  $F=8.5$ ,  $Df=12$ ), TPSL REPK p212 ( $p=0.029$ ,  $F=4.6$ ,  $Df=15$ ), TPSL REPK p217 ( $p=0.036$ ,  $F=4.6$ ,  $Df=15$ ), and pIGST ( $p=0.018$ ,  $F=14.7$ ,  $Df=5$ ). Significance was determined via one-way ANOVA with Tukey posthoc test. Data are represented as mean  $\pm$  SD.

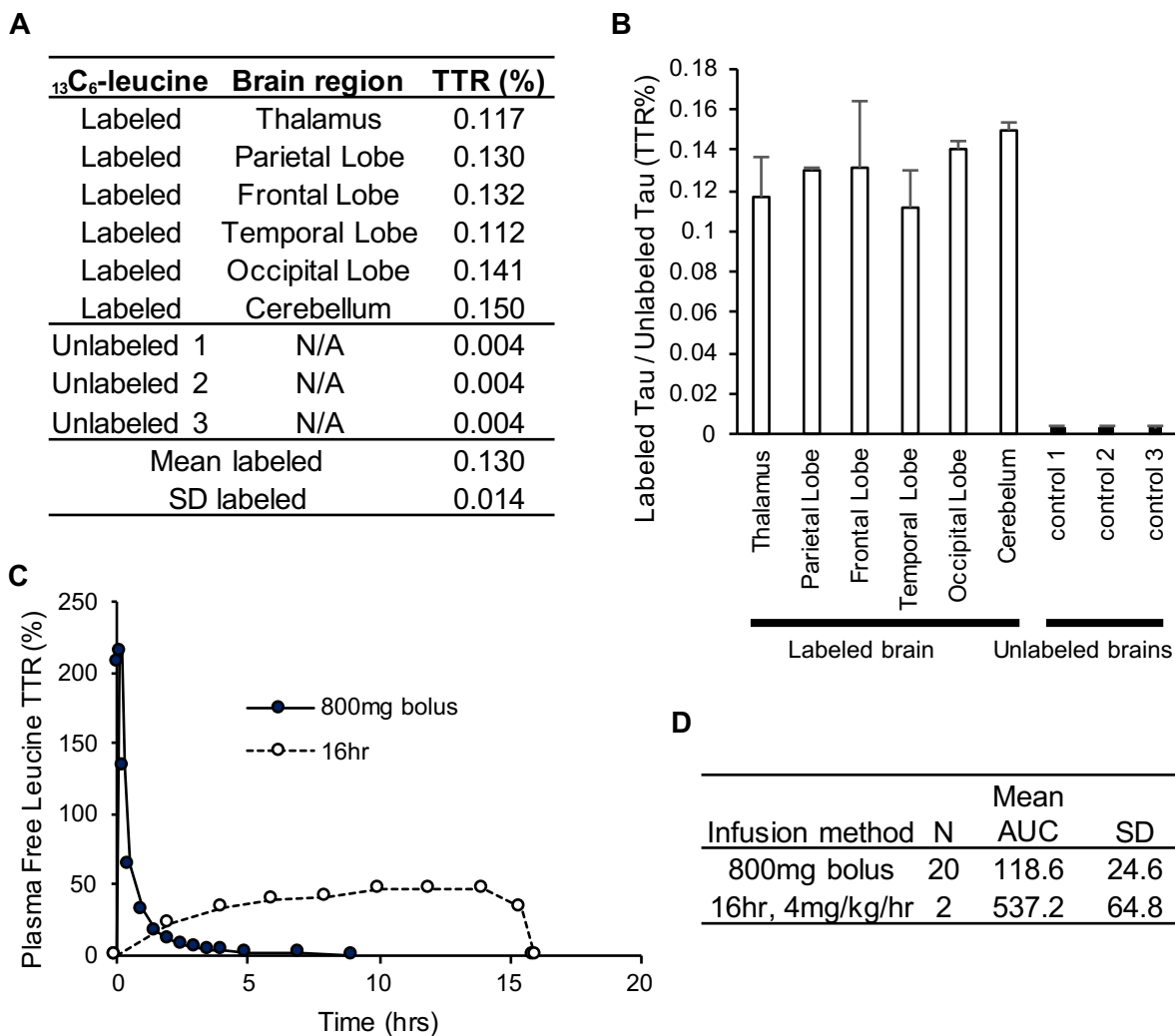


**Figure S6. Labeling of Tau in the Human Brain Related to Figure 3.** (A) Summary table describing the labeling (TTR%) of three control brains and a brain donated by a participant who had 800mg bolus infusion eight days before passing away. (B) Quantitation of (A). Data are represented as mean  $\pm$  SD. (C) Examples of plasma free leucine curves obtained from 800mg bolus infusion and 16hr 4mg/kg/hr infusion. (D) Summary of Area Under the Curve (AUC) obtained from plasma free leucine measurements from 20 participants who received 800mg bolus infusion and 2 participants who received 16hr infusion. Plasma leucine from the participant who passed away 8 days from 800mg bolus infusion was not available. Thus, average AUC from 20 participants were used for normalization in **Figure 3G**.

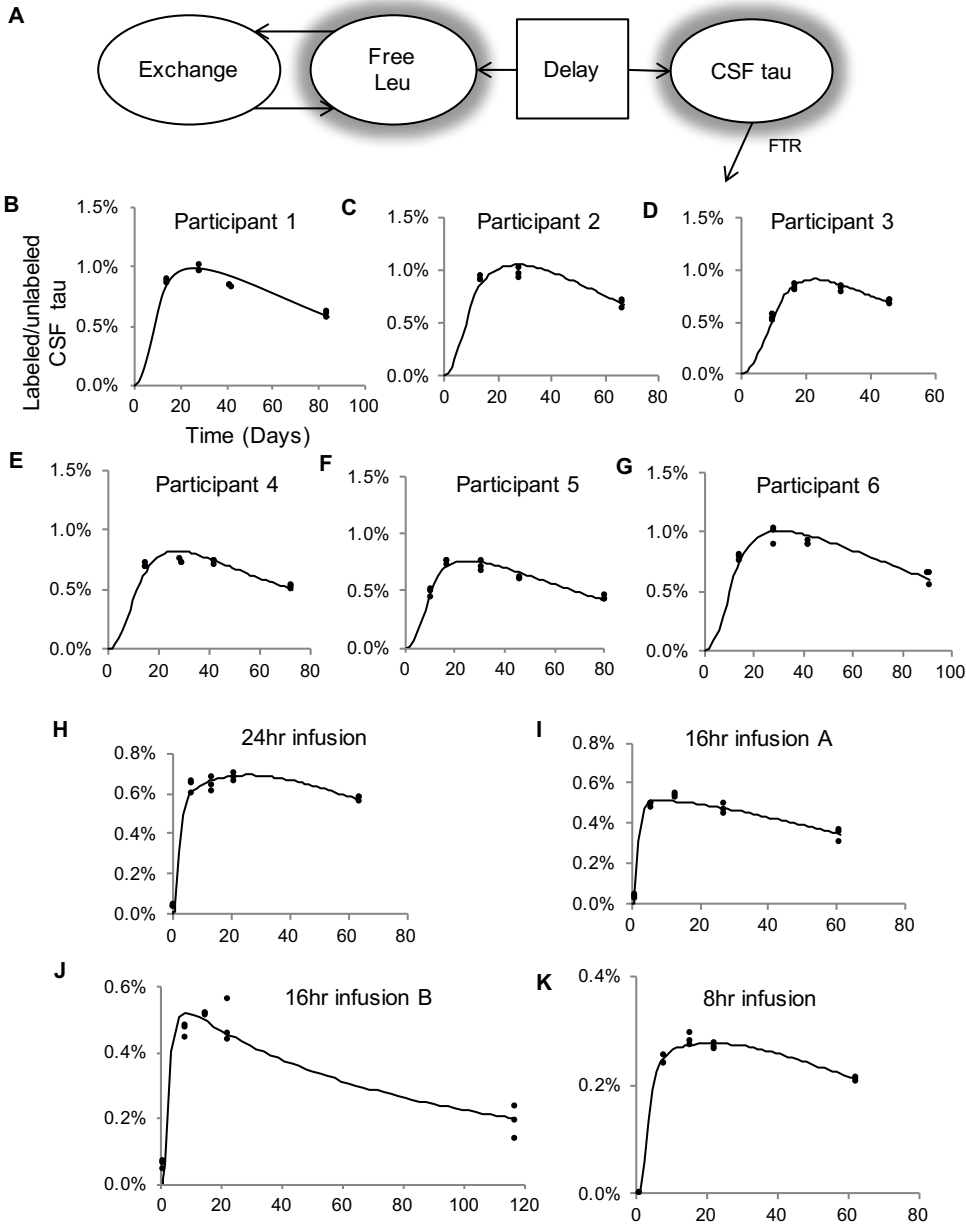


**Figure S7. Compartmental modeling of  $^{13}\text{C}_6$ -leucine labeling in healthy participants.**

**Related to Figure 3.** (A) The model consists of a 2-compartment system to represent the free  $^{13}\text{C}_6$ -leucine enrichment time course, a delay element, and CSF tau. The fractional turnover rate (FTR) of tau is optimized to fit the shape of the CSF tau enrichment time course. The model fits to the labeling of CSF tau of the six orally labeled participants (B-G) and four infusion participants (H-K).

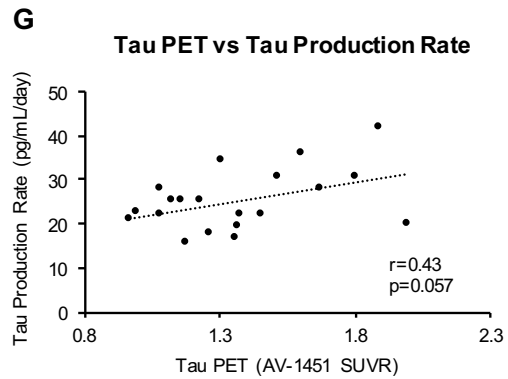
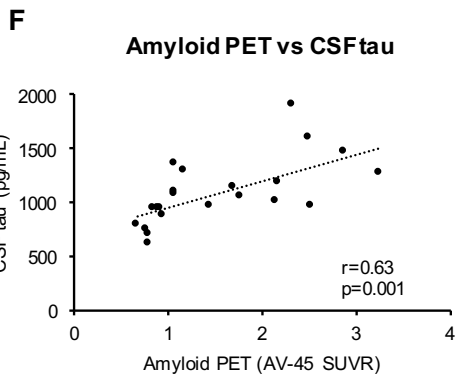
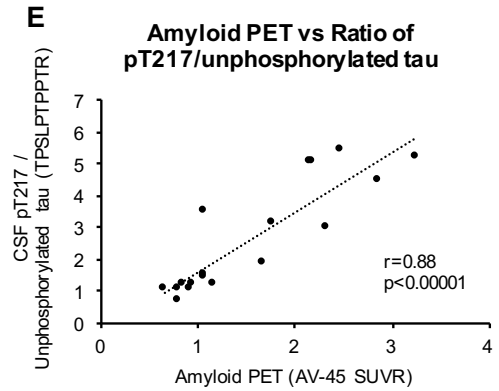
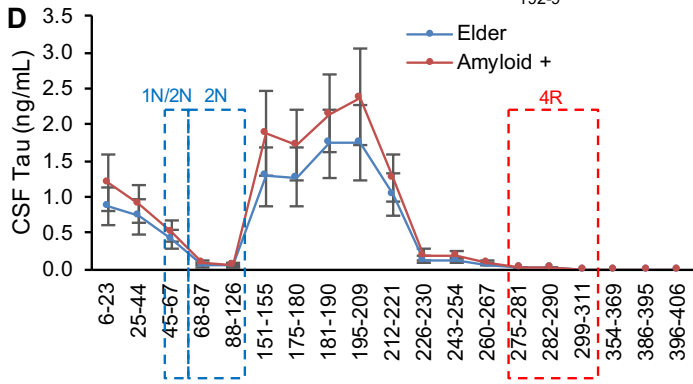
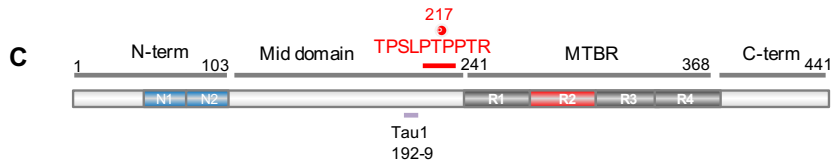
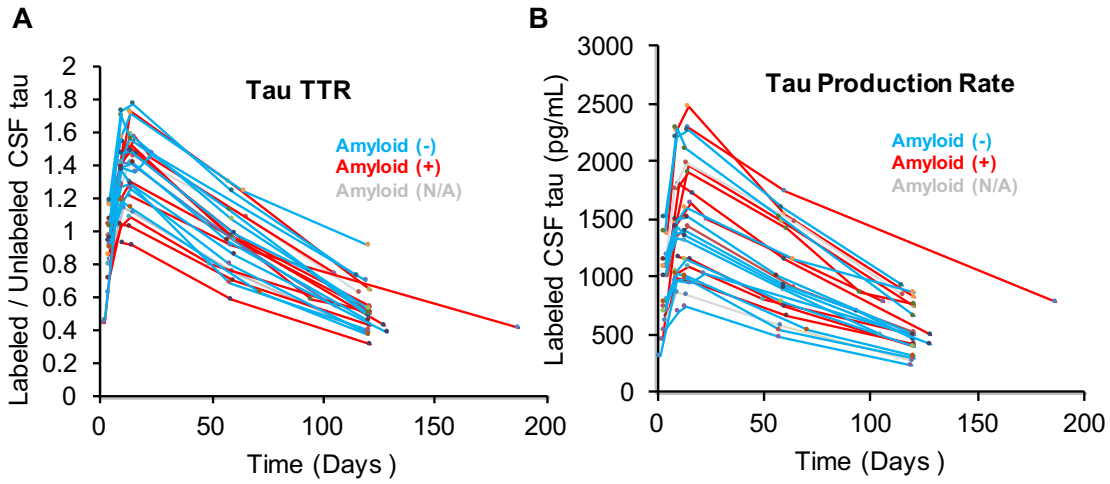


**Figure S8. Tau kinetics curves from 24 participants with and without Alzheimer's pathology. Related to Figure 4.** (A) Tau kinetics curves shown by the ratio of labeled/unlabeled tau over time, normalized by the amount of leucine received (plasma free leucine). (B) Absolute concentration of labeled CSF tau over time. Cut-off of amyloid PET (AV-45 SUVR) = 1.22 was used to determine amyloid positivity. (C) Schematic of the longest tau isoform (2N4R), the epitope of Tau1 antibody, T<sub>PSLPTTPR</sub> peptide and phosphorylation at T217. (D) CSF tau profile is similar across the protein in amyloid positive (+) and negative Elder group (Age 61-87). Data are represented as mean  $\pm$  SD. (E) The ratio of phosphorylated tau at T217 (pT217) and unphosphorylated tau (T<sub>PSLPTPPTR</sub> peptide) positively correlates with amyloid PET. (F) The correlation between pT217/tau ratio and amyloid PET ( $r=0.88$ ) is greater than that of CSF tau absolute concentration and amyloid PET ( $r=0.63$ ). (G) Tau PET positively correlates with Tau production rate. Spearman correlation ( $r$  and  $p$  value) was calculated to determine each association.